

SCIENTIFIC REPORTS

OPEN

Active modulation of the calcifying fluid carbonate chemistry ($\delta^{11}\text{B}$, B/Ca) and seasonally invariant coral calcification at sub-tropical limits

Claire L. Ross^{1,2}, James L. Falter^{1,2} & Malcolm T. McCulloch^{1,2}

Coral calcification is dependent on both the supply of dissolved inorganic carbon (DIC) and the up-regulation of pH in the calcifying fluid (cf). Using geochemical proxies ($\delta^{11}\text{B}$, B/Ca, Sr/Ca, Li/Mg), we show seasonal changes in the pH_{cf} and DIC_{cf} for *Acropora yongei* and *Pocillopora damicornis* growing *in-situ* at Rottnest Island (32°S) in Western Australia. Changes in pH_{cf} range from 8.38 in summer to 8.60 in winter, while DIC_{cf} is 25 to 30% higher during summer compared to winter ($\times 1.5$ to $\times 2$ seawater). Thus, both variables are up-regulated well above seawater values and are seasonally out of phase with one another. The net effect of this counter-cyclical behaviour between DIC_{cf} and pH_{cf} is that the aragonite saturation state of the calcifying fluid (Ω_{cf}) is elevated ~4 times above seawater values and is ~25 to 40% higher during winter compared to summer. Thus, these corals control the chemical composition of the calcifying fluid to help sustain near-constant year-round calcification rates, despite a seasonal seawater temperature range from just ~19° to 24 °C. The ability of corals to up-regulate Ω_{cf} is a key mechanism to optimise biomineralization, and is thus critical for the future of coral calcification under high CO_2 conditions.

Coral reefs face an uncertain future due to increasing seawater temperatures and ocean acidification resulting from CO_2 -driven climate change^{1,2}. Rising ocean temperatures are expected to lead to more frequent mass coral bleaching events, defined as a loss of the endosymbiotic dinoflagellates (zooxanthellae) from the coral host^{3–5}. While corals have demonstrated the capacity to adapt to long-term changes in climate, they are still extremely vulnerable to abrupt warming events (i.e., weeks to months) as evident, for example, by the mass bleaching events that often follow El Niño-Southern Oscillation (ENSO) driven warming events^{6,7}. Additionally, evidence suggests^{8–10} that declining seawater pH will cause the growth rates of important marine calcifiers, such as hermatypic corals, to slow down. The effect of declining pH on the calcification process is however still in question, as corals possess the physiological mechanisms to partially resist or limit the effects of ocean acidification on the bio-calcification process^{11–16}. They accomplish this through the up-regulation of the pH of the calcifying fluid (pH_{cf}); a process that likely occurs via active ionic exchange of Ca^{2+} with H^+ via Ca-ATPase^{17,18} ‘pumps’ at the site of calcification^{11–16}. This in turn helps to elevate the aragonite saturation state in the calcifying fluid (Ω_{cf}), a key requirement for the formation of their calcium carbonate (CaCO_3) skeletons^{11–16,19,20}. In addition to up-regulating pH_{cf} , corals supply the calcifying fluid with metabolically generated dissolved inorganic carbon (DIC)¹⁸. This raises the activity of carbonate ions within the calcifying fluid ($[\text{CO}_3^{2-}]_{\text{cf}}$) and, therefore, increases Ω_{cf} ²¹. Thus, corals manipulate rates of aragonite precipitation by actively elevating both pH_{cf} and DIC_{cf} ²¹.

Despite the importance of internal carbonate chemistry in determining rates of mineral precipitation, temperature is still the main factor influencing the rates of coral growth^{22–24}. This is due to both the strong temperature-dependent rate kinetics of aragonite precipitation²⁵ as well as the sensitivity of coral physiology to extremes in temperature^{6,26}. For example, calcification rates in tropical corals are generally thought to follow a Gaussian-shaped curve whereby calcification increases as temperature increases until an optimum is reached; after this maximum, rates decline with increasing temperature^{7,24,27}. Light is also an important driver of coral calcification on both diurnal and seasonal timescales, with rates of carbon fixation by the zooxanthellae

¹Oceans Institute and School of Earth Sciences, The University of Western Australia, Perth, Australia. ²Australian Research Council Centre of Excellence for Coral Reef Studies, The University of Western Australia, Perth, Australia. Correspondence and requests for materials should be addressed to C.L.R. (email: claire.ross@research.uwa.edu.au)

Variable	Units	Description
$\delta^{11}\text{B}$	‰	Boron isotope
pH_{cf}	—	pH of the calcifying fluid
pH_{T}	—	pH on the total hydrogen ion scale
pH_{sw}	—	pH of the seawater
DIC_{cf}	$\mu\text{mol kg}^{-1}$	Dissolved inorganic carbon in the calcifying fluid
DIC_{sw}	$\mu\text{mol kg}^{-1}$	Dissolved inorganic carbon in the seawater
Ω_{cf}	—	Aragonite saturation state of the calcifying fluid
Ω_{sw}	—	Aragonite saturation state of the seawater
T	°C	Temperature
B/Ca	mmol mol^{-1}	Boron to calcium ratio
Li/Mg	mmol mol^{-1}	Lithium to magnesium ratio
Sr/Ca	mmol mol^{-1}	Strontium to calcium ratio

Table 1. Nomenclature. Definition of variables used in this paper.

symbiont being light dependent^{18,28,29}. Therefore, it is not surprising that higher rates of coral calcification are generally found in summer compared to winter^{24,30–35}. These findings^{24,30–35} are consistent with the assumption that during the summer there are higher rates of metabolically-derived carbon supply to the coral¹⁸ and enhanced temperature-driven precipitation kinetics²⁵.

A recent study by Ross *et al.*³⁶, however, found that calcification rates for the reef-building species *Acropora yongei* and *Pocillopora damicornis* growing offshore Western Australia (Rottneest Island, 32°S) exhibited minimal seasonality and, in fact, exhibited similar or even higher rates in winter. The authors suggested that this uncharacteristic seasonal pattern in calcification rates was due to increased nutrient uptake in winter^{36–38} and/or a possible sub-lethal stress response in summer^{36,39}. Another possibility, which is explored herein, is that corals physiologically manipulate the chemistry of their calcifying fluid to enhance rates of calcification. Earlier studies have demonstrated that the biological mediation of pH up-regulation can modulate rates of calcification^{11,13,14,16}. However, our ability to infer both aspects of the carbonate chemistry (i.e., pH and DIC) under *in-situ* conditions has only recently become possible via measuring the boron isotopic composition ($\delta^{11}\text{B}$)^{40–42} and elemental abundance of boron (B/Ca)⁴³ in coral skeletons. Furthermore, while other methods of interrogating the carbonate chemistry of the calcifying fluid have been developed and provide some informative results^{14,15,19,28,44}, they generally must be conducted under tightly constrained laboratory conditions that differ greatly from the *in-situ* ‘natural’ reef habitats in which corals grow. Nonetheless, previous studies have shown that estimates of internal coral pH_{cf} derived from geochemical tracers^{12,13,40,45} are consistent with more direct measurements^{14,19,44}, affirming that boron isotopes are providing unbiased measurements of pH at the site of calcification. With these new developments^{12,21,40,45}, we can now determine how the carbonate chemistry of the calcifying fluid (pH_{cf} , DIC_{cf} , Ω_{cf}) responds to natural and seasonally varying changes in light, temperature and seawater pH. We show that quantifying these relationships is critical to understanding and predicting how coral growth will respond to man-made climate change under real-world conditions.

Here we examine seasonal changes in the carbonate chemistry of the calcifying fluid (pH_{cf} , DIC_{cf} and Ω_{cf}) for branching corals, *Acropora yongei* and *Pocillopora damicornis*, sampled every 1 to 2 months for three summers and two winters in Salmon Bay, Rottneest Island (32°S), Western Australia (WA). Boron isotopic compositions ($\delta^{11}\text{B}$) are used as a proxy for pH_{cf} and are combined with skeletal B/Ca ratios to determine $[\text{CO}_3^{2-}]_{\text{cf}}$ and hence DIC_{cf} . We show that corals in this sub-tropical environment seasonally elevate Ω_{cf} to levels that are ~4 times higher than ambient seawater and ~25% higher in winter compared to summer. We also find enhanced rates of skeletal precipitation relative to that expected from inorganic rate kinetics²⁵; thus emphasizing the ability of corals to manipulate their internal carbonate chemistry to promote biomineralization.

Results

Coral habitat. Monthly average water temperatures at Salmon Bay ranged from 19.3° to 23.7°C during this study period, giving a seasonal range of 4.4°C (Supplementary Fig. S1). Monthly mean light levels increased from a minimum of just 15 mol m⁻² d⁻¹ in winter to a maximum of 48 mol m⁻² d⁻¹ in summer (Supplementary Table S1). Weekly average measured seawater pH_{T} at Rottneest Island showed minimal variability (<0.05 pH units) between summer (January 2014) and winter (July 2014; see Supplementary Fig. S2). The definitions for all physical and biogeochemical variables are provided in Table 1.

Internal skeletal carbonate chemistry. Coral skeletal Li/Mg and Sr/Ca ratios show significant inverse relationships with seasonal increases in temperature for both *A. yongei* ($r^2 = 0.82$, $r^2 = 0.76$, respectively, $p < 0.001$ for both; Fig. 1) and for *P. damicornis* ($r^2 = 0.71$, $r^2 = 0.73$, respectively, $p < 0.001$ for both; Fig. 1; Supplementary Table S2). Thus, the geochemical composition of the apical section of the coral skeleton analysed confirms that coral skeletal growth was the same time as when ambient seawater chemistry was measured. This excellent agreement is further supported by earlier measurements³⁶ showing that these coral colonies grew ~4 mm month⁻¹.

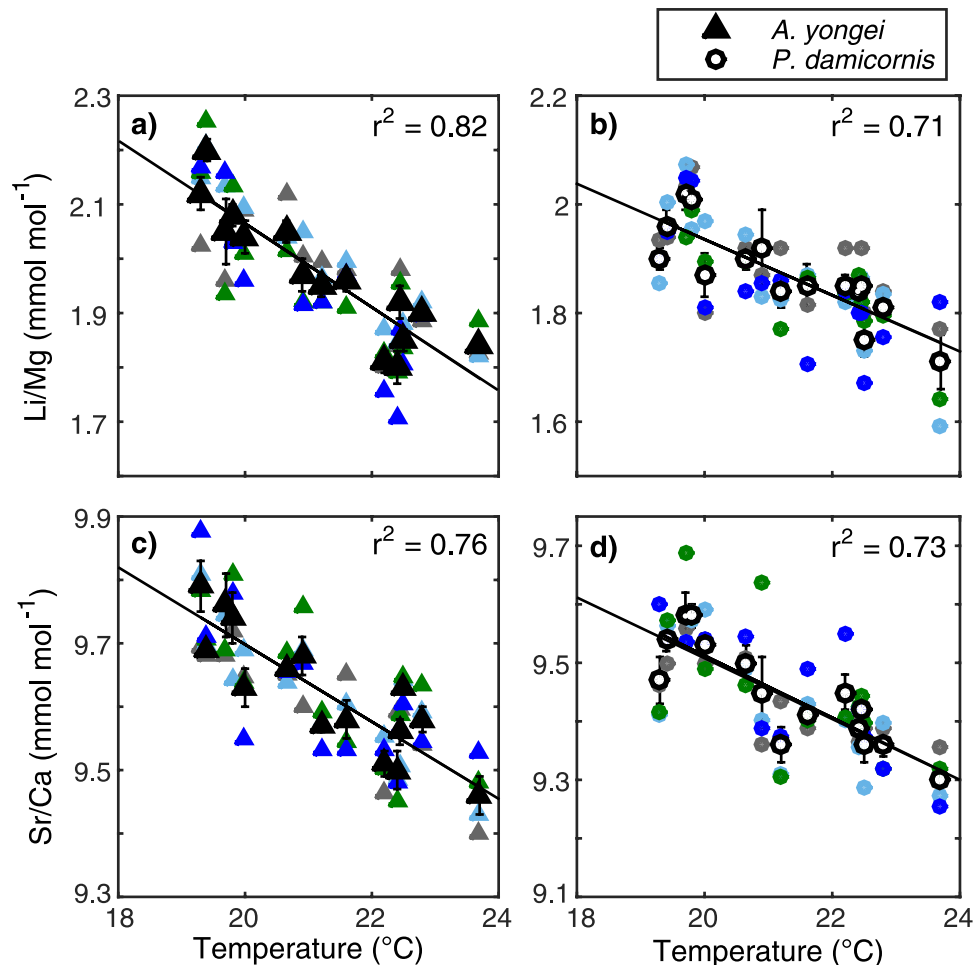


Figure 1. Measured Li/Mg and Sr/Ca in corals at Rottneet Island plotted against seawater temperature. (a,b) Li/Mg plotted against temperature with regression equation $\text{Li/Mg} = -0.08T_{\text{sw}} + 3.63$ for *Acropora yongei* and $\text{Li/Mg} = -0.05T_{\text{sw}} + 2.99$ for *Pocillopora damicornis* (c,d) Sr/Ca plotted against temperature with regression equation $\text{Sr/Ca} = -0.061T_{\text{sw}} + 10.92$ for *Acropora yongei*, and $\text{Sr/Ca} = -0.053T_{\text{sw}} + 10.57$ for *Pocillopora damicornis*. Coloured symbols represent each colony while the black symbols with lines denote the mean (± 1 SE; $n = 4$) for each time point.

Seasonal $\delta^{11}\text{B}$ varies by up to 2.7‰ between the warmest month (23.7°C) and the coolest month (19.3°C), ranging from a minimum of 22.0‰ in February for both species to a maximum of 24.9‰ in August for *A. yongei* and 24.8‰ for *P. damicornis* (Fig. 2a,b; Supplementary Table S2). These ranges in $\delta^{11}\text{B}$ correspond to seasonal variations in derived pH_{cf} of 8.38 (summer) to 8.60 (winter) for both *A. yongei* and *P. damicornis* (Fig. 3) with a lower $\Delta\text{pH}_{\text{cf}}$ of 0.28 ($\Delta\text{pH}_{\text{cf}} = \text{pH}_{\text{cf}} - \text{pH}_{\text{sw}}$) corresponding to warmer seawater temperatures and a higher $\Delta\text{pH}_{\text{cf}}$ of 0.50 corresponding to cooler seawater temperatures (Fig. 3). Skeletal ratios of boron to calcium (B/Ca) range from 0.49 to 0.59 mmol mol^{-1} for *A. yongei* and 0.59 to 0.74 mmol mol^{-1} for *P. damicornis* (Fig. 2c,d; Supplementary Table S2). These B/Ca ratios correspond to carbonate ion concentrations within the calcifying fluid $[\text{CO}_3^{2-}]_{\text{cf}}$ of from 806 to 973 $\mu\text{mol kg}^{-1}$ for *A. yongei*, and 645 to 886 $\mu\text{mol kg}^{-1}$ for *P. damicornis* (Supplementary Table S3) and are ~20 to 40% higher at their peak in winter compared to their low in summer. These values fall within the range of other tropical corals as reported using carbonate-sensitive microelectrodes under laboratory conditions (600 to 1550 $\mu\text{mol kg}^{-1}$)⁴⁴.

The DIC_{cf} derived from the B/Ca ratio proxy is 1.5 to 2 times higher than ambient seawater and is positively correlated with seasonal changes in seawater temperature ($r^2 = 0.38$, $p = 0.015$ for *A. yongei* and $r^2 = 0.37$, $p = 0.017$ for *P. damicornis*; Fig. 4). The DIC_{cf} in both coral species is also 25 to 30% higher in summer compared to winter (4520 $\mu\text{mol kg}^{-1}$ in summer vs. 3620 $\mu\text{mol kg}^{-1}$ in winter for *A. yongei* and 3700 $\mu\text{mol kg}^{-1}$ in summer vs. ~2900 $\mu\text{mol kg}^{-1}$ in winter for *P. damicornis*; Fig. 3b). There is a counter-cyclical relationship between DIC_{cf} and pH_{cf} such that seasonal changes in DIC_{cf} are negatively correlated with seasonal changes in pH_{cf} ($r^2 = 0.64$, $p = 0.002$ for *A. yongei* and $r^2 = 0.39$, $p = 0.01$ for *P. damicornis*; Supplementary Fig. S3). As a result of this inverse relationship between DIC_{cf} and pH_{cf} , the highest Ω_{cf} occurs in winter (16.2 for *A. yongei* and 14.9 for *P. damicornis*; Fig. 3d) and lowest in summer (13.0 for *A. yongei* and 10.4 for *P. damicornis*; Fig. 3d). Thus, Ω_{cf} is negatively correlated with seasonal changes in temperature ($r^2 = 0.37$, $p = 0.015$ and $r^2 = 0.37$, $p = 0.02$ for *A. yongei* and *P.*

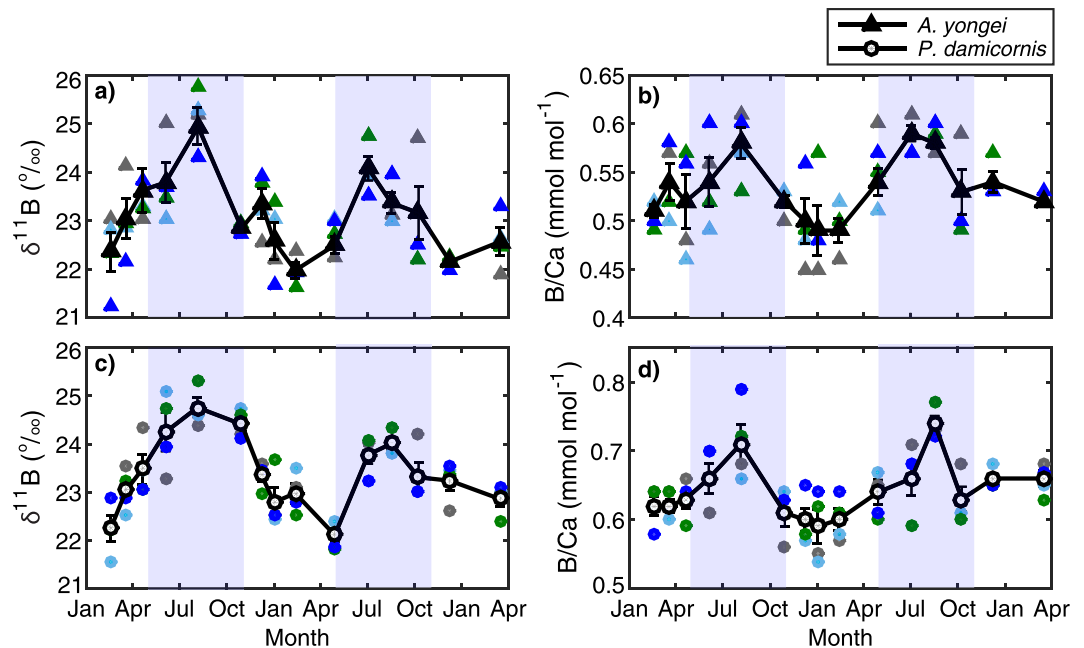


Figure 2. Seasonal changes in the boron isotopic signature and boron to calcium ratio (B/Ca) of corals at Rottneet Island. (a,b) Seasonal time-series of $\delta^{11}\text{B}$ (‰) and (c,d) boron to calcium ratios (B/Ca) for all four colonies sampled of *Acropora yongei* and *Pocillopora damicornis*. Coloured symbols represent each colony while the black symbols with lines denote the mean ± 1 SE ($n = 4$) for each time point. Light blue shading denotes winter and unshaded areas denote summer, defined based on seasonal changes in temperature and light.

damicornis, respectively; Fig. 4). Due to the up-regulation of both DIC_{cf} and pH_{cf} , Ω_{cf} is roughly 3.5 to 5 times higher than the mean annual seawater aragonite saturation state ($\Omega_{\text{sw}} \approx 3.2$) depending on taxa and season.

Coral growth rates. Results from Ross *et al.*³⁶ demonstrated that calcification rates generally deviated from their long-term (>1 year) average growth rates of $1.6 \text{ mg cm}^{-2} \text{ d}^{-1}$ for *A. yongei* and $0.67 \text{ mg cm}^{-2} \text{ d}^{-1}$ for *P. damicornis* by just $\pm 20\%$ to $\pm 30\%$ over the 18-month period, respectively (Table 2)³⁶. These calcification rates were either negatively correlated with temperature for *P. damicornis* ($r^2 = 0.45$) or showed little or no seasonal coherency for *A. yongei* (i.e., no correlation with temperature $r^2 = 0.015$)³⁶. Thus, calcification rates exhibited unexpected seasonal patterns whereby they were, on average, similar across seasons for *A. yongei*, and slightly higher in winter compared to summer for *P. damicornis*.

Discussion

Here we show that corals living in a sub-tropical environment have the ability to modulate rates of calcification by seasonally counter-regulating pH_{cf} and DIC_{cf} to elevate Ω_{cf} . The ability to infer coral pH_{cf} from $\delta^{11}\text{B}$ isotopic measurements is supported by measurements from microelectrodes^{19,28} and pH-sensitive dyes^{13,14,46}. For example, previous studies^{13,14} have shown that pH_{cf} up-regulation is ~ 0.6 to 2 units above seawater values in the light. Results from $\delta^{11}\text{B}$ -derived pH_{cf} generally fall within this range and are broadly consistent⁴⁶ with these measurements (~ 0.3 to 0.6 pH units above seawater)^{11–13,16,20}, given that they are integrated over multiple weeks of biomineralization. Additional variability between methods (i.e., geochemical proxies and direct measurements) may also result from the different species used and the conditions under which the measurements are conducted⁴⁷. More recent, albeit limited, measurements of the carbonate ion concentration using microelectrodes report values of 600 to $1550 \text{ } \mu\text{mol kg}^{-1}$ in the calcifying fluid⁴⁴. These instantaneous measurements performed under laboratory conditions, while providing some informative results, have significant limitations. For instance, microelectrode measurements are currently unable to determine the dynamic seasonal interactions between components of the coral calcifying fluid carbonate chemistry (pH_{cf} , DIC_{cf} , Ω_{cf}) documented here under naturally fluctuating conditions. This is due to the limitations of existing technology, as measurements must be conducted using separate probes for pH_{cf} and $[\text{CO}_3^{2-}]_{\text{cf}}$ and under highly controlled laboratory conditions. Thus, our findings highlight the importance of $\delta^{11}\text{B}$ and B/Ca proxies as a method for inferring the internal carbonate chemistry in corals under real-world conditions and over longer (i.e., seasonal) time scales.

Laboratory experiments have nevertheless demonstrated that coral pH_{cf} typically shows a relatively consistent linear and muted response to changes in pH_{sw} , such that changes in coral pH_{cf} are usually equal to approximately one-third to one-half of those in pH_{sw} ^{12,14,47–51}. Thus, according to the results of those experiments, seasonal changes in coral pH_{cf} should have been on the order of ~ 0.02 pH units, due to the relatively small seasonal variability in pH_{sw} at Rottneet Island (~ 0.07 ; Supplementary Fig. S2). In contrast, seasonal variations in pH_{cf} are an order of magnitude higher (> 0.2 pH units). Therefore, our results unequivocally demonstrate that seawater pH is not the major factor driving seasonal changes in coral pH_{cf} up-regulation in this study.

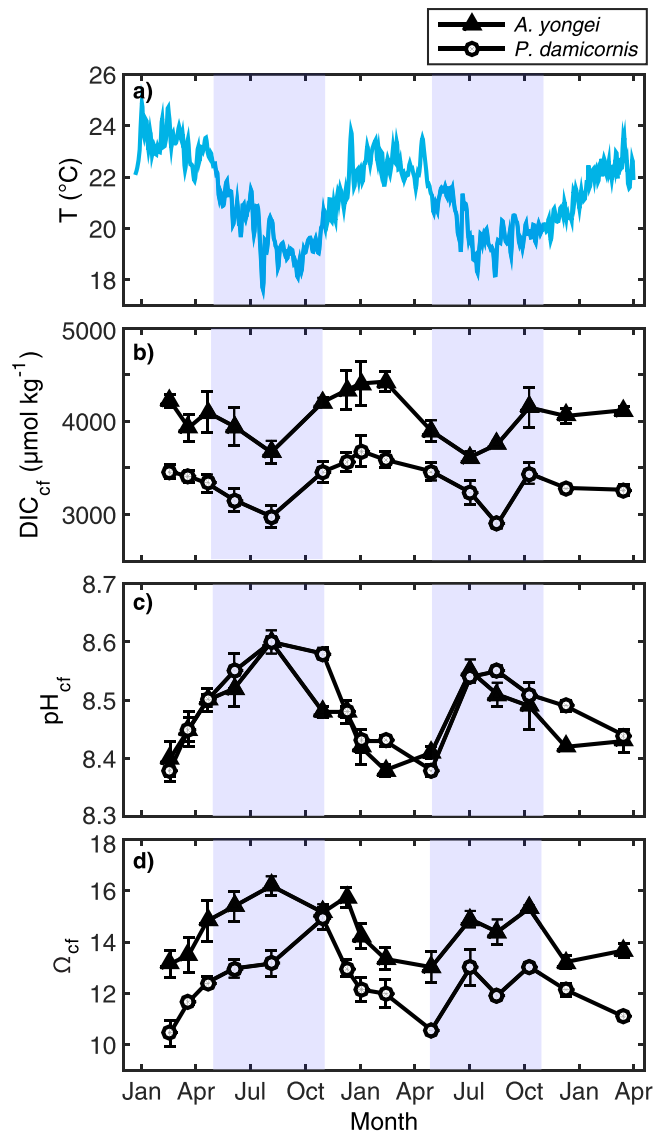


Figure 3. Time-series of seasonal changes in seawater temperature and calcifying fluid parameters (DIC_{cf} , pH_{cf} , Ω_{cf}). (a) Seawater temperature (b) pH_{cf} , (c) predicted dissolved inorganic carbon (DIC_{cf}), and (d) Ω_{cf} for coral the species *Acropora yongei* and *Pocillopora damicornis* averaged (± 1 SE) over each growth period. Light blue shading denotes winter and unshaded areas denote summer, defined based on seasonal changes in temperature and light.

Our current understanding of the sensitivity of the calcifying fluid chemical composition to changes in seawater carbonate chemistry has generally been inferred from controlled laboratory experiments^{14,47–51}, which have kept other environmental conditions constant, such as temperature^{14,47–51} and/or light^{14,50,51}. However, our findings demonstrate that other environmental factors beyond pH_{sw} may have a much larger influence on pH_{cf} and $[\text{CO}_3^{2-}]_{\text{cf}}$ at least on seasonal time-scales. For instance, the observed inverse relationship between seasonally varying pH_{cf} and DIC_{cf} is suggestive of a deliberate mechanism to compensate for seasonal declines in temperature and light, and thus changes to the supply and/or transport of DIC necessary for coral growth²¹. The lower levels of DIC in the calcifying fluid during winter reflect a reduction in rates of carbon fixation by endosymbionts in winter and are compensated for by higher pH_{cf} up-regulation (Fig. 3). Despite the stabilizing effects that a counter-cyclical seasonal relationship between pH_{cf} and DIC_{cf} would have on Ω_{cf} , we nonetheless show that Ω_{cf} also varies seasonally. This seasonal behaviour of Ω_{cf} may, at the very least, dampen any expected seasonality in rates of coral calcification.

To better constrain the relative sensitivity of coral calcification rates to seasonal changes in both temperature and the carbonate chemistry of the calcifying fluid, calcification rates were modelled using the inorganic rate equation (see Eq. 5 in Methods)¹². In this model, aragonite precipitation occurs according to abiotic rate kinetics under chemical conditions dictated by the living coral (e.g., elevated pH_{cf} and DIC_{cf}). Three scenarios are considered: (1) temperature and Ω_{cf} vary with season, (2) temperature, DIC_{cf} and Ω_{cf} vary with season while pH_{cf} is calculated based on seawater pH_{sw} in accordance with the results of fixed aquaria experiments^{40,49}, and (3) Ω_{cf}

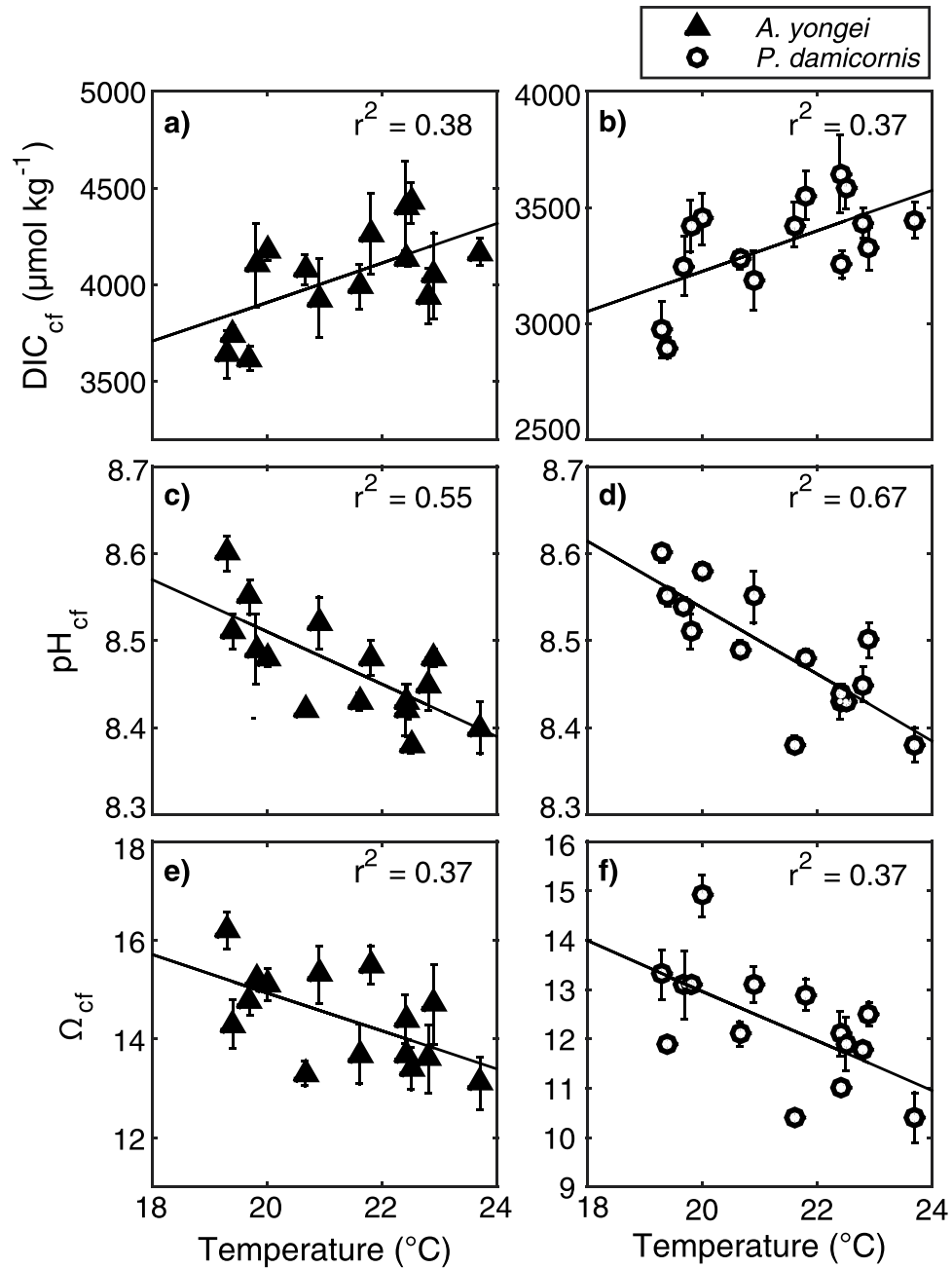


Figure 4. Relationships between calcifying fluid parameters versus seawater temperature. (a,b) Seasonal changes in DIC_{cf}, (c,d) pH_{cf}, and (e,f) Ω_{cf} with seawater temperatures for *Acropora yongei* and *Pocillopora damicornis* averaged (±1 SE) over each growth period.

varies with season, but temperature is kept constant at its annual average (21.7°C). Modelled rates of calcification based on inorganic rate kinetics are a factor of 2 to 7 times lower than the measured calcification rates (see Supplementary Table S4). This indicates that an estimated Ω_{cf} of 30 to 50 is required to attain the measured rates of calcification and thus much higher than our seasonal range of ~10 to 16, depending on taxa (Fig. 3d). Thus, physiological mechanisms must be operative in enhancing rates of skeletal precipitation relative to that expected from inorganic rate kinetics.

During summer, the higher DIC_{cf} supply is offset by a systematic reduction in pH_{cf} to modulate Ω_{cf} and calcification rates. While the estimated calcification rates from inorganic rate kinetics in scenario 1 are still ~50% higher at the peak in summer compared to the minima in winter, this seasonal change is nevertheless substantially less than the estimated ~90% seasonal change in calcification rates if pH_{cf} levels were more or less constant year-round, as inferred from fixed condition aquaria experiments. Calcification rates estimated from both scenarios indicate that the seasonal variation in the measured coral calcification rates should be pro-cyclical with temperature and much greater than observed³⁶ (Fig. 5). Thus, scenarios 1 and 2, which allow for the full seasonal variation in temperature to be expressed through the inorganic rate kinetics, exhibit large deviations from the

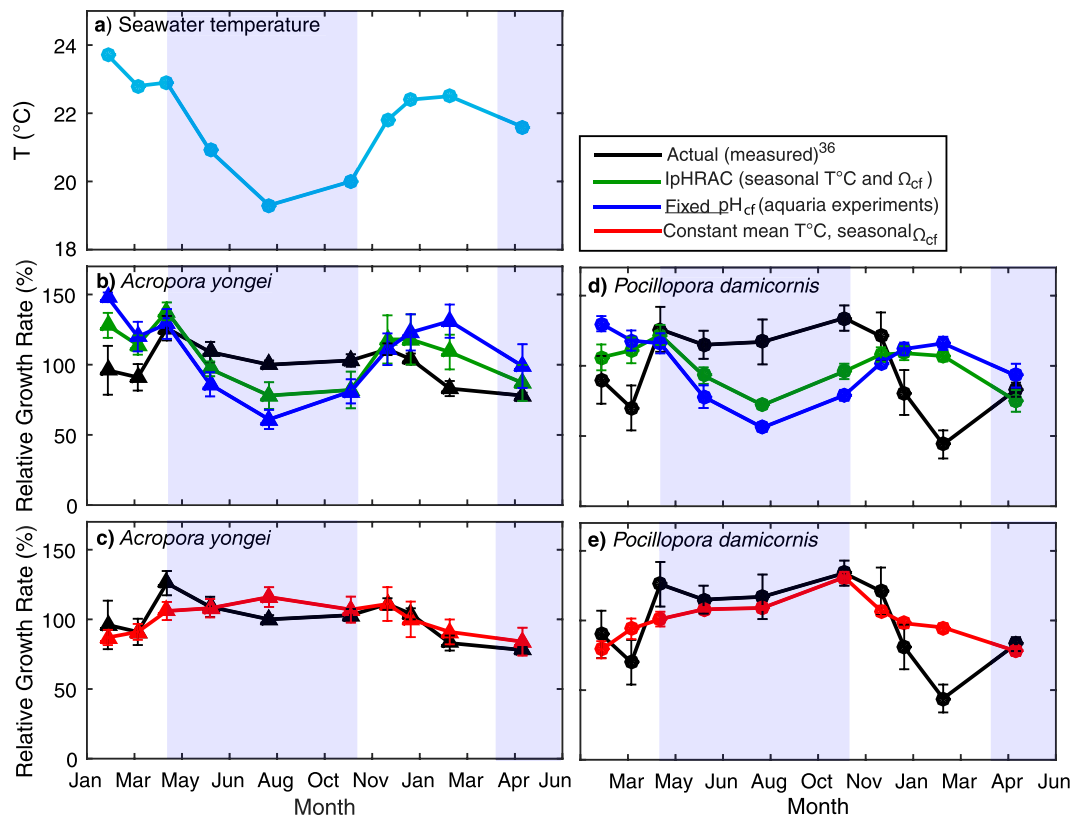


Figure 5. Measured and modelled seasonal growth rate response for branching *Acropora yongei* and *Pocillopora damicornis* at Rottneest Island. (a) Seasonal changes in average seawater temperature (°C). Actual calcification rates measured using the buoyant weight technique³⁶ and predicted calcification rates modelled using inorganic rate kinetics for (b,c) *A. yongei*, and (d,e) *P. damicornis*. Black symbols represent the measured calcification rates (mean \pm 1 SE) for *A. yongei* ($n = 16$) and *P. damicornis* ($n = 9$)³⁶. Green symbols represent the predicted calcification rates using seasonally varying temperature and seasonally varying Ω_{cf} , blue symbols represent the predicted calcification rates using pH_{cf} calculated from fixed condition experiments for *Acropora* spp., ($y = 0.51pH_{sw} + 4.28$ ^{40,49}; where pH_{sw} ranged from 8.03–8.10), and red symbols represent the predicted rates using a constant mean temperature (21.7°C) and seasonally varying Ω_{cf} . All growth rates are expressed as percentage relative to the mean. Light blue shading denotes winter and unshaded areas denote summer, defined based on seasonal changes in temperature and light.

measured calcification rates for *A. yongei* (Scenario 1: RMSE = 17.0%; Scenario 2: RMSE = 30.3%), and *P. damicornis* (Scenario 1: RMSE = 32.7%; Scenario 2: RMSE = 43.3%). There is a strong physiological control over Ω_{cf} such that calcification rates appear to be modulated more by Ω_{cf} rather than temperature directly. We find that the calcification rates modelled under a constant mean temperature (i.e., scenario 3) show the best fit to the observed seasonal patterns in calcification (RMSE = 11.5% and 20.8%, respectively; Fig. 5). One possibility is that differences between the complex skeletal micro-architecture of coral growth (e.g., a higher active surface area on which precipitation can occur)¹⁵ compared to abiotic aragonite crystal formation could result in the enhanced rates of biologically-mediated coral calcification shown here. Another possibility is that other factors may influence seasonal patterns in rates of calcification, for example, changes in the speed at which the corals create organic matrices and crystal templates^{52–56} necessary for mineralization. This cannot be ruled out given that the calcification rate measurements are integrated over several weeks of biomineralization.

Although the relatively seasonally invariant calcification rates for corals from Rottneest Island stand in contrast with findings from more tropical environments^{24,33–35}, there are also a number of studies^{36,39,57,58} that show limited seasonal variability in calcification rates for several coral species. These studies were conducted across a range of locations (i.e., spanning 10 degrees latitude) in Western Australia, and are thus widely applicable to reef-building corals growing in a various environments. There have been a number of hypotheses to explain this lack of seasonality, ranging from the residual effects of sub-lethal thermal stress following an unusually strong marine heat wave³⁹, to higher rates of particulate nutrient uptake in winter^{36,37,57}. In the present study, however, the limited seasonal variability in calcification rates can be explained by the seasonally counter-cyclical up-regulation of pH_{cf} and DIC_{cf} to deliberately elevate Ω_{cf} and support near-constant rates of calcification year-round, despite much cooler temperatures during winter. This apparent physiological control over the internal carbonate chemistry is further supported by the results from the Papua New Guinea CO₂ seeps¹⁶ and Free Ocean Carbon Enrichment

Species	Summer 2013		Winter 2013				Summer 2014			Winter 2014	Ref
	Feb	Mar	Apr	Jun	Aug	Oct	Dec	Jan	Feb	Apr	
<i>Acropora yongei</i>	1.54 ± 0.28	1.46 ± 0.15	2.02 ± 0.14	1.76 ± 0.12	1.61 ± 0.05	1.66 ± 0.07	1.79 ± 0.07	1.67 ± 0.06	1.33 ± 0.09	1.25 ± 0.03	36
<i>Pocillopora damicornis</i>	0.60 ± 0.12	0.47 ± 0.10	0.84 ± 0.10	0.77 ± 0.07	0.79 ± 0.11	0.90 ± 0.06	0.81 ± 0.12	0.54 ± 0.11	0.30 ± 0.07	0.55 ± 0.03	36

Table 2. Coral calcification rates at Rottneest Island. Seasonal changes in rates of calcification ($\text{mg cm}^{-2} \text{d}^{-1}$; mean \pm SE) for coral species (a) *Acropora yongei*, and (b) *Pocillopora damicornis*³⁶. Italic denotes winter and roman areas denote summer.

experiment (FOCE)¹¹; both of which demonstrated the mechanism of pH_{cf} ‘homeostasis’ in corals despite exposure to extreme variations in ambient pH_{sw} .

We have now identified a key mechanism of chemical regulation within the calcifying fluid composition that assists reef-building coral to calcify year-round in sub-tropical conditions (i.e., lower and more seasonally variable temperature and light). While these findings are based on branching corals at Rottneest Island, they nevertheless demonstrate a key physiological mechanism whereby changes in the calcifying fluid carbonate chemistry act to modulate calcification rates. Although such robust regulation of chemical conditions during calcification will help protect the growth of adult corals from the influence of declining seawater pH ^{12,15}, it will not necessarily preclude corals from being vulnerable to thermal stress⁵⁹. Thus, the future survival of coral reefs in the face of Earth’s rapidly changing climate will ultimately depend on the capacity of reef-building coral to endure the increasingly frequent and intense CO_2 -driven warming events⁵⁹.

Methods

Overview. This study was conducted at Salmon Bay on the south side of Rottneest Island, which is located approximately 20 km west of Perth, WA (32°S, 115°E). See Ross *et al.*³⁶ for a detailed map of study area. Single individual branches of *A. yongei* and *P. damicornis* were collected from four naturally growing colonies (1 branch per colony) every 1 to 3 months between February 2013 and March 2015 and subject to the geochemical analyses described herein.

Environmental data. Continuous measurements of seawater pH_{T} (Total scale, with ± 0.03 accuracy) were made using a SeaFET ocean pH sensor (Satlantic, Canada) in October 2014 (spring) and April 2015 (autumn). Earlier measurements were made in July 2013 (winter) and February 2014 (summer)³⁶. Seawater temperature was continuously measured at the study site for the entire duration of the study using HOBO temperature loggers ($\pm 0.2^\circ\text{C}$, Onset Computer Corp.). Daily down-welling planar photo-synthetically active radiation (PAR in $\text{mol m}^{-2} \text{d}^{-1}$) was measured from December 2013 to July of 2014 using Odyssey light loggers ($\pm 5\%$, Odyssey Data Recording) that had been calibrated against a high-precision LiCor 192 A cosine PAR ($\pm 5\%$, LiCor Scientific) sensor³⁶. For this location, seasons were defined as follows: winter from mid-April through to mid-October and summer from mid-November through to mid-April.

Boron isotopic and trace element analyses. The $\delta^{11}\text{B}$ of coral skeletons were measured from the uppermost apical section of the growing tip of *A. yongei* and *P. damicornis* skeletons (Supplementary Fig. S4, Supplementary Table S5). We sampled ~ 4 mm of the apical growing tip based on our previous study³⁶ showing average monthly extension rates of ~ 50 mm yr^{-1} (or ~ 4 mm month^{-1}). Alternate methods for determining the sclero-chronology of the deposited skeletal material include using fluorescent staining⁶⁰ or isotope labelling, which are informative for analysis by laser ablation-multi-collector-ICP-MS⁶¹. Unfortunately, repeated labelling of the coral colonies used in this study was not feasible due to the frequent (1 to 3 month) skeletal sampling resolution and long study period (i.e., ~ 2 years). Instead, we used molar ratios of strontium to calcium (Sr/Ca) and lithium to magnesium (Li/Mg) in the most recently deposited skeletal material and well-known, highly correlated relationships between these trace element ratios and ambient seawater temperature⁶² to confirm the seasonal chronology of skeletal growth histories¹¹.

Powders derived from the temporally controlled samples of coral skeleton were cleaned⁶³ and dissolved in 0.58 N HNO_3 . Aliquots of these acidified samples were analysed for trace elements (Sr/Ca, Li/Mg, and B/Ca) using an X-Series 2 Quadrupole Inductively Coupled Plasma Mass Spectrometer (Thermo Fisher Scientific). The extraction and concentration of boron-rich solutions from acidified sample solutions was performed via paired cation-anion resin columns and analysed with a NU Plasma II (Nu Instruments, Wrexham, UK) multi-collector inductively coupled plasma mass spectrometer (MC-ICPMS)⁶⁴.

Boron isotope pH-proxy. We determined the pH of the calcifying fluid from the measured $\delta^{11}\text{B}$ values according to the following equation⁶⁵:

$$\text{pH}_{\text{cf}} = \frac{\text{p}K_{\text{B}} - \text{Log}\{[\delta^{11}\text{B}_{\text{sw}} - \delta^{11}\text{B}_{\text{carb}}]\}}{[\alpha_{\text{B}}\delta^{11}\text{B}_{\text{carb}} - \delta^{11}\text{B}_{\text{sw}} + 1000(1.0272 - 1)]} \quad (1)$$

where $\text{p}K_{\text{B}}$ is the dissociation constant of boric acid in seawater⁶⁶ at the temperature and salinity of the seawater in Salmon Bay, $\delta^{11}\text{B}_{\text{carb}}$ and $\delta^{11}\text{B}_{\text{sw}}$ are the boron isotopic composition of the coral skeleton and average seawater, respectively, and α_{B} is the isotopic fractionation factor (1.0272)⁶⁷.

Estimation of DIC_{cf} and modelled rates of mineral precipitation. We estimate the concentration of carbonate ions at the site of calcification ($[\text{CO}_3^{2-}]_{cf}$) using molar ratios of boron to calcium (B/Ca) according to the following relationship⁴⁵ simplified by McCulloch, *et al.*²¹:

$$[\text{CO}_3^{2-}]_{cf} = \frac{[\text{B}(\text{OH})_4^-]_{cf} K_D^{B/\text{Ca}}}{[\text{B}/\text{Ca}]_{arag}} \quad (2)$$

where $[\text{B}(\text{OH})_4^-]_{cf}$ is the concentration of borate in the calcifying fluid, $K_D^{B/\text{Ca}}$ is the molar distribution coefficient for boron in aragonite, and $[\text{B}/\text{Ca}]_{arag}$ is the elemental ratio of boron to calcium in the coral skeleton. To estimate $[\text{B}(\text{OH})_4^-]_{cf}$ we assume that the concentration of total inorganic boron in the calcifying fluid is salinity dependent^{68,69}, and equal to that of the surrounding seawater. The strong linear relationship between the calculated $[\text{CO}_3^{2-}]_{cf}$ (using eq. 2) and the measured $[\text{CO}_3^{2-}]_{cf}$ from abiogenic experiments by Holcomb, *et al.*⁴⁵ is shown in Supplementary Fig. S5. The relative amounts of borate are determined by the pH_{cf} ⁶⁶, as determined from the $\delta^{11}\text{B}$ isotopic measurements (see eq. 1). The $K_D^{B/\text{Ca}}$ is calculated as a function of pH_{cf} according to^{21,45}:

$$K_D^{B/\text{Ca}} = 0.00297 \exp(-0.0202 [\text{H}^+]_{cf}) \quad (3)$$

where $[\text{H}^+]$ in the calcifying fluid is estimated from the coral $\delta^{11}\text{B}$ derived pH_{cf} and only varies by less than $\pm 3\%$ over the range in which most coral pH_{cf} are known to occur (8.3 to 8.6)²¹.

The concentration of DIC_{cf} is then calculated from pH_{cf} (eq. 1) and $[\text{CO}_3^{2-}]_{cf}$ (eq. 2).

The Ω_{cf} is estimated from $[\text{Ca}^{2+}]$ and $[\text{CO}_3^{2-}]$ (from $\delta^{11}\text{B}$ and B/Ca) according to the following relationship:

$$\Omega_{cf} = \frac{[\text{Ca}^{2+}][\text{CO}_3^{2-}]}{K_{sp}^*} \quad (4)$$

where K_{sp}^* is the solubility constant for aragonite as a function of temperature and salinity and $[\text{Ca}^{2+}]$ is assumed to be the same as the surrounding seawater values.

Finally, we used the combination of Ω_{cf} and temperature to infer rates of abiotic aragonite precipitation (G) at the site of calcification according to the model of internal pH-regulation abiotic calcification model (IpHRAC)¹²:

$$G = k(\Omega_{cf} - 1)^n \quad (5)$$

where k and n are temperature-dependent empirical constants²⁵.

Observed rates of coral calcification. Calcification rates ($\text{mg CaCO}_3 \text{ cm}^{-2} \text{ d}^{-1}$) for both *A. yongei* ($n = 16$) and *P. damicornis* ($n = 9$) were measured³⁶ on individual coral colonies (mounted on plastic tiles and deployed *in-situ*) using the buoyant weight technique^{70,71}. These calcification measurements were conducted on colonies from the same location and at the same time as when branches were collected (from separate colonies) for the analysis of skeletal geochemistry. This field-based approach allowed the comparison of seasonal changes of *in-situ* determined coral calcification rates³⁶ with concomitant changes in seawater temperature, pH and DIC together with coral calcifying fluid pH_{cf} and DIC_{cf}.

Availability of data. Data is available at the Zenodo Digital Repository (DOI: [10.5281/zenodo.1009710](https://doi.org/10.5281/zenodo.1009710)).

References

1. Feely, R. A. *et al.* Impact of anthropogenic CO_2 on the CaCO_3 system in the oceans. *Science* (80). **305**, 362–366 (2004).
2. Orr, J. *et al.* Anthropogenic ocean acidification over the twenty-first century and its impact on calcifying organisms. *Nature* **437**, 681–6 (2005).
3. van Hooijdonk, R. & Huber, M. Effects of modeled tropical sea surface temperature variability on coral reef bleaching predictions. *Coral Reefs* **31**, 121–131 (2012).
4. Donner, S. D., Skirving, W. J., Little, C. M., Oppenheimer, M. & Hoegh-Guldberg, O. Global assessment of coral bleaching and required rates of adaptation under climate change. *Glob Chang. Biol.* **11**, 2251–2265 (2005).
5. Hoegh-Guldberg, O. Climate change, coral bleaching and the future of the world's coral reefs. *Mar. Freshw. Res.* **50**, 839 (1999).
6. Schoepf, V., Stat, M., Falter, J. L. & McCulloch, M. T. Limits to the thermal tolerance of corals adapted to a highly fluctuating, naturally extreme temperature environment. *Sci. Rep.* **5**, 17639 (2015).
7. Sawall, Y. *et al.* Extensive phenotypic plasticity of a Red Sea coral over a strong latitudinal temperature gradient suggests limited acclimatization potential to warming. *Sci. Rep.* **5**, 8940 (2015).
8. Marubini, F., Ferrier-Pages, C. & Cuif, J.-P. Suppression of skeletal growth in scleractinian corals by decreasing ambient carbonate concentration: a cross-family comparison. *Proc. Biol. Sci.* **270**, 179–84 (2003).
9. Langdon, C. Effect of elevated pCO_2 on photosynthesis and calcification of corals and interactions with seasonal change in temperature/irradiance and nutrient enrichment. *J. Geophys. Res.* **110**, C09S07 (2005).
10. Kuffner, I. B., Andersson, A. J., Jokiel, P. L., Rodgers, K. S. & Mackenzie, F. T. Decreased abundance of crustose coralline algae due to ocean acidification. *Nat. Geosci.* **1**, 114–117 (2008).
11. Georgiou, L. *et al.* pH homeostasis during coral calcification in a free ocean CO_2 enrichment (FOCE) experiment, Heron Island reef flat, Great Barrier Reef. *Proc. Natl. Acad. Sci.* 201505586. <https://doi.org/10.1073/pnas.1505586112> (2015)
12. McCulloch, M. T., Falter, J. L., Trotter, J. & Montagna, P. Coral resilience to ocean acidification and global warming through pH up-regulation. *Nat. Clim. Chang.* **2**, 1–5 (2012).
13. Holcomb, M. *et al.* Coral calcifying fluid pH dictates response to ocean acidification. *Sci. Rep.* **4**, 5207 (2014).
14. Venn, A., Tambutté, É., Holcomb, M., Allemand, D. & Tambutté, S. Live tissue imaging shows reef corals elevate pH under their calcifying tissue relative to seawater. *PLoS One* **6**, e20013 (2011).
15. Venn, A. A., Tambutté, É., Holcomb, M., Laurent, J. & Allemand, D. Impact of seawater acidification on pH at the tissue–skeleton interface and calcification in reef corals. *PNAS* **110**, 1634–1639 (2013).

16. Wall, M. *et al.* Internal pH regulation facilitates *in situ* long-term acclimation of massive corals to end-of-century carbon dioxide conditions. *Sci. Rep.* 1–7, <https://doi.org/10.1038/srep30688> (2016).
17. McConnaughey, T. A. Ion transport and the generation of biomineral supersaturation in the 7th International Symposium Biomineralization (ed. Allemand, D. & Cuif, J.-P.) 1–18 (1994).
18. Allemand, D. *et al.* Biomineralisation in reef-building corals: from molecular mechanisms to environmental control. *Comptes Rendus Palevol* 3, 453–467 (2004).
19. Ries, J. B. A physicochemical framework for interpreting the biological calcification response to CO₂-induced ocean acidification. *Geochim. Cosmochim. Acta* 75, 4053–4064 (2011).
20. Tanaka, K. *et al.* Response of *Acropora digitifera* to ocean acidification: constraints from $\delta^{11}\text{B}$, Sr, Mg, and Ba compositions of aragonitic skeletons cultured under variable seawater pH. *Coral Reefs*, <https://doi.org/10.1007/s00338-015-1319-6> (2015).
21. McCulloch, M. T., D'Olivo Cordero, J., Falter, J. L. & Holcomb, M. Coral calcification in a changing World and the interactive dynamics of pH and DIC up-regulation. *Nat. Commun.*
22. Veron, J. Corals in space and time: the biogeography and evolution of the Scleractinia. *University of New South Wales Press*, Ithaca, Sydney, 321 (Cornell Univ. Press, Ithaca, 1995).
23. Lough, J. & Barnes, D. Environmental controls on growth of the massive coral. *Porites*. *J Exp Mar Biol Ecol* 245, 225–243 (2000).
24. Marshall, A. T. & Clode, P. Calcification rate and the effect of temperature in a zooxanthellate and an azooxanthellate scleractinian reef coral. *Coral Reefs* 23, 218–224 (2004).
25. Burton, E. A. & Walter, L. M. Relative precipitation rates of aragonite and Mg calcite from seawater: Temperature or carbonate ion control? *Geology* 15, 111 (1987).
26. Grotoli, A. G. *et al.* The cumulative impact of annual coral bleaching can turn some coral species winners into losers. *Glob. Chang. Biol.* 20, 3823–3833 (2014).
27. Jokiel, P. & Coles, S. L. Effects of Temperature on the Mortality and Growth of Hawaiian Reef Corals *. *Mar Biol* 208, 201–208 (1977).
28. Al-Horani, F., Al-Moghrabi & de Beer, D. The mechanism of calcification and its relation to photosynthesis and respiration in the scleractinian coral *Galaxea fascicularis*. *Mar Biol* 142, 419–426 (2003).
29. Schneider, K., Levy, O., Dubinsky, Z. & Erez, J. *In situ* diel cycles of photosynthesis and calcification in hermatypic corals. *Limnol Oceanogr.* 54, 1995–2002 (2009).
30. Crossland, C. Seasonal variations in the rates of calcification and productivity in the coral *Acropora formosa* on a high-latitude reef. *Mar Ecol Prog Ser* 15, 135–140 (1984).
31. Rodolfo-Metalpa, R., Martin, S., Ferrier-Pagès, C. & Gattuso, J.-P. Response of the temperate coral *Cladocora caespitosa* to mid- and long-term exposure to pCO₂ and temperature levels projected in 2100. *Biogeosci Discuss* 6, 7103–7131 (2009).
32. Kuffner, I. B., Hickey, T. D. & Morrison, J. M. Calcification rates of the massive coral *Siderastrea siderea* and crustose coralline algae along the Florida Keys (USA) outer-reef tract. *Coral Reefs* 32, 987–997 (2013).
33. Venti, A., Andersson, A. & Langdon, C. Multiple driving factors explain spatial and temporal variability in coral calcification rates on the Bermuda platform. *Coral Reefs* 33, 979–997 (2014).
34. Roik, A., Roder, C., Röthig, T. & Voolstra, C. R. Spatial and seasonal reef calcification in corals and calcareous crusts in the central Red Sea. *Coral Reefs* 35 (2015).
35. Vajed Samiei, J. *et al.* Variation in calcification rate of *Acropora downingi* relative to seasonal changes in environmental conditions in the northeastern Persian Gulf. *Coral Reefs*. <https://doi.org/10.1007/s00338-016-1464-6> (2016).
36. Ross, C. L., Falter, J. L., Schoepf, V. & McCulloch, M. T. Perennial growth of hermatypic corals at Rottneest Island, Western Australia (32°S). *PeerJ* 3, e781 (2015).
37. Wyatt, A. S. J., Falter, J. L., Lowe, R. J., Humphries, S. & Waite, A. M. Oceanographic forcing of nutrient uptake and release over a fringing coral reef. *Limnol. Oceanogr.* 57, 401–419 (2012).
38. Houlbrèque, F., Tambutté, E., Richard, C. & Ferrier-pagès, C. Importance of a micro-diet for scleractinian corals. *Mar Ecol Prog Ser* 282, 151–160 (2004).
39. Foster, T., Short, J., Falter, J. L., Ross, C. & McCulloch, M. T. Reduced calcification in Western Australian corals during anomalously high summer water temperatures. *J Exp Mar Biol Ecol* 461, 133–143 (2014).
40. Trotter, J. *et al.* Quantifying the pH 'vital effect' in the temperate zooxanthellate coral *Cladocora caespitosa*: Validation of the boron seawater pH proxy. *Earth Planet. Sci. Lett.* 303, 163–173 (2011).
41. Wei, H., Jiang, S., Xiao, Y. & Hemming, N. G. Boron isotopic fractionation and trace element incorporation in various species of modern corals in Sanya Bay, South China Sea. *J. Earth Sci.* 25, 431–444 (2014).
42. Pelejero, C. *et al.* Preindustrial to modern interdecadal variability in coral reef pH. *Science* 309, 2204–7 (2005).
43. Allison, N., Cohen, I., Finch, A., Erez, J. & Tudhope, A. W. Corals concentrate dissolved inorganic carbon to facilitate calcification. *Nat. Commun.* 5, 5741 (2014).
44. Cai, W.-J. *et al.* Microelectrode characterization of coral daytime interior pH and carbonate chemistry. *Nat. Commun.* 7, 11144 (2016).
45. Holcomb, M., DeCarlo, T. M., Gaetani, G. A. & McCulloch, M. T. Factors affecting B/Ca ratios in synthetic aragonite. *Chem. Geol.* 437, 67–76 (2016).
46. Gagnon, A. C. Coral calcification feels the acid. *Proc. Natl. Acad. Sci. USA* 110, 1567–8 (2013).
47. Hönisch, B. *et al.* Assessing scleractinian corals as recorders for paleo-pH: Empirical calibration and vital effects. *Geochim. Cosmochim. Acta* 68, 3675–3685 (2004).
48. Marubini, F., Barnett, H., Langdon, C. & Atkinson, M. J. Dependence of calcification on light and carbonate ion concentration for the hermatypic coral *Porites compressa*. *Mar Ecol Prog Ser* 220, 153–162 (2001).
49. Reynaud, S., Hemming, N. G., Juillet-Leclerc, A. & Gattuso, J.-P. Effect of pCO₂ and temperature on the boron isotopic composition of the zooxanthellate coral *Acropora sp.* *Coral Reefs* 539–546 (2004).
50. Marubini, F., Ferrier-Pagès, C., Furla, P. & Allemand, D. Coral calcification responds to seawater acidification: a working hypothesis towards a physiological mechanism. *Coral Reefs* 27, 491–499 (2008).
51. Krief, S. *et al.* Physiological and isotopic responses of scleractinian corals to ocean acidification. *Geochim. Cosmochim. Acta* 74, 4988–5001 (2010).
52. Tambutté, S. *et al.* Characterization and role of carbonic anhydrase in the calcification process of the azooxanthellate coral *Tubastrea aurea*. *Mar. Biol.* 151, 71–83 (2007).
53. Mass, T. *et al.* Cloning and characterization of four novel coral acid-rich proteins that precipitate carbonates *in vitro*. *Curr. Biol.* 23, 1126–1131 (2013).
54. Tambutté, E. *et al.* Morphological plasticity of the coral skeleton under CO₂-driven seawater acidification. *Nat. Commun.* 6, 7368 (2015).
55. Clode, P. L. & Marshall, A. T. Calcium associated with a fibrillar organic matrix in the scleractinian coral *Galaxea fascicularis*. *Protoplasma* 220, 153–161 (2003).
56. Falini, G., Fermani, S. & Goffredo, S. Coral biomineralization: A focus on intra-skeletal organic matrix and calcification. *Semin. Cell Dev. Biol.* 46, 17–26 (2015).
57. Falter, J. L., Lowe, R. J., Atkinson, M. J. & Cuet, P. Seasonal coupling and de-coupling of net calcification rates from coral reef metabolism and carbonate chemistry at Ningaloo Reef, Western Australia. *J Geophys Res* 117, C05003 (2012).

58. Dandan, S. S., Falter, J. L., Lowe, R. J. & McCulloch, M. T. Resilience of coral calcification to extreme temperature variations in the Kimberley region, northwest Australia. *Coral Reefs*, <https://doi.org/10.1007/s00338-015-1335-6> (2015).
59. Hoegh-Guldberg, O. *et al.* Coral reefs under rapid climate change and ocean acidification. *Science* (80-). **318**, 1737–1742 (2007).
60. Holcomb, M., Cohen, A. L. & McCorkle, D. C. An evaluation of staining techniques for marking daily growth in scleractinian corals. *J. Exp. Mar. Bio. Ecol.* **440**, 126–131 (2013).
61. Fietzke, J. *et al.* Boron isotope ratio determination in carbonates via LA-MC-ICP-MS using soda-lime glass standards as reference material. *J. Anal. At. Spectrom.* **25**, 1953–1957 (2010).
62. Montagna, P. *et al.* Li/Mg systematics in scleractinian corals: Calibration of the thermometer. *Geochim. Cosmochim. Acta* **132**, 288–310 (2014).
63. Holcomb, M. *et al.* Cleaning and pre-treatment procedures for biogenic and synthetic calcium carbonate powders for determination of elemental and boron isotopic compositions. *Chem. Geol.* **398**, 11–21 (2015).
64. McCulloch, M. T., Holcomb, M., Rankenburg, K. & Trotter, J. A. Rapid, high-precision measurements of boron isotopic compositions in marine carbonates. *Rapid Commun. mass Spectrom.* **RCM 28**, 2704–12 (2014).
65. Zeebe, R. & Wolf-Gladrow, D. CO₂ in Seawater: Equilibrium, Kinetics, Isotopes in *Elsevier Oceanography Series* (Ed. Richard, E. Z., Dieter, W.G.) **65**, 1–84 (Elsevier Science, 2001).
66. Dickson, A. G. Thermodynamics of the dissociation of boric acid in synthetic seawater from 273.15 to 318.15 K. *Deep Sea Res. Part A. Oceanogr. Res. Pap.* **37**, 755–766 (1990).
67. Klochko, K., Kaufman, A. J., Yao, W., Byrne, R. H. & Tossell, J. A. Experimental measurement of boron isotope fractionation in seawater. *Earth Planet. Sci. Lett.* **248**, 261–270 (2006).
68. Foster, G. L., Pogge von Strandmann, P. A. E. & Rae, J. W. B. Boron and magnesium isotopic composition of seawater. *Geochemistry, Geophys. Geosystems* **11**, 1–10 (2010).
69. Lewis, E., Wallace, D. & Allison, L. Program Developed for CO₂ System Calculations (Oak Ridge National Laboratory, 1998).
70. Bak, R. Coral weight increment *in situ*. A new method to determine coral growth. *Mar Biol* **20**, 45–49 (1973).
71. Jokiel, P., Maragos, J. & Franzisket, L. Coral growth: buoyant weight technique in *Coral reefs: research methods* (ed. Stoddart, D. & Johannes, R. E.) 529–542 (UNESCO, 1978).

Acknowledgements

Thanks to A. Comeau, K. Rankenburg, M. Holcomb and J. Pablo D’Olivo for training and assistance in the coral isotope and mass spectrometry laboratories. We are grateful to H. Clarke, T. Foster, S. Dandan, V. Schoepf, B. Vaughan, and K. Williams for assisting on field trips. We also thank the staff at Rottneest Island Authority for their support of our fieldwork. This research was supported by funding provided by an ARC Laureate Fellowship (LF120100049) awarded to Professor M. McCulloch, the ARC Centre of Excellence for Coral Reef Studies (CE140100020), and an Australian Post Graduate Scholarship awarded to C. Ross.

Author Contributions

C.R. designed the experiments, conducted the experiments, analyzed the data and wrote the manuscript. J.F. conducted the experiments, analyzed the data, and wrote the manuscript. M.M. designed the experiments, analyzed the data, and wrote the manuscript.

Additional Information

Supplementary information accompanies this paper at <https://doi.org/10.1038/s41598-017-14066-9>.

Competing Interests: The authors declare that they have no competing interests.

Publisher's note: Springer Nature remains neutral with regard to jurisdictional claims in published maps and institutional affiliations.



Open Access This article is licensed under a Creative Commons Attribution 4.0 International License, which permits use, sharing, adaptation, distribution and reproduction in any medium or format, as long as you give appropriate credit to the original author(s) and the source, provide a link to the Creative Commons license, and indicate if changes were made. The images or other third party material in this article are included in the article's Creative Commons license, unless indicated otherwise in a credit line to the material. If material is not included in the article's Creative Commons license and your intended use is not permitted by statutory regulation or exceeds the permitted use, you will need to obtain permission directly from the copyright holder. To view a copy of this license, visit <http://creativecommons.org/licenses/by/4.0/>.

© The Author(s) 2017